Downloaded 09/11/14 to 98.201.57.71. Redistribution subject to SEG license or copyright; see Terms of Use at http://library.seg.org/

Rock Physics Modeling of Organic-rich Shales with Different Maturity Levels

Xuan Qin, De-hua Han, and Luanxiao Zhao, Rock Physics Lab, University of Houston*

Summary

In this study, we develop rock physics models to simulate the elastic properties of organic-rich shales with different maturity levels. The modeling results of immature and mature shales match well with the measured data from the Bakken shale samples (Vernik and Liu, 1997). It also suggests that higher maturity level and higher total organic carbon (TOC) both yield lower Vp/Vs ratio and stronger anisotropy. When TOC is high, we find that the elastic responses of organic-rich shales are mainly determined by maturity level. However, when TOC is low, TOC mainly controls the elastic properties of organic-rich shales.

Introduction

Organic-rich shale formations develop in a complex way. Initially, organic matter and mud-sized (< 62.5μm) particles are transported in suspension, whose elastic properties follows the Reuss bound and has a Poisson's ratio of 0.5. These particles settle out of suspension and begin to compact. New sediments deposited on the older sediments compact the underlying particles and cause the sheet-like particles to preferentially align, which contributes to shale's intrinsic anisotropy. With the increase of burial depth and temperature, the dehydration of clay minerals occurs and shale's shear modulus increases. Compaction can dramatically reduce the porosity of shale; chemical cementation can also lower porosity and permeability (Dræge et al., 2006). When the geological environment satisfies the condition of maturation, hydrocarbons can be generated through a series of decomposition reactions (Luo and Vasseur, 1996; Carcione and Gangi, 2000), from which we can classify the process of maturation into three levels (Vanorio et al., 2008), i.e. immature, mature, and overmature. In the immature stage, kerogen with a vitrinite reflectance (Ro, %) less than 0.6 can decompose to form oil and little gas, when it is heated to over 50°C. In the mature stage [0.6 < Ro (%) < 1.3], generated oil can continue crack to gas, when it is heated to over 110°C approximately. In the overmature stage [Ro (%) > 1.3], the generated solid residue can decompose to form gas and the final solid product graphite, when it is heated to over 180°C.

It is difficult to characterize organic-rich shales because of the organic matter as well as its maturation during burial sedimentation. Some authors have applied different methods to predict and analyze shale's properties. Carcione et al. (2011) found a significant dependence of velocity on total organic carbon (TOC) when modeling oil-saturated rock using the Backus average as well as the Krief/Gassmann models. Vernik and Milovac (2011), and Zhu et al. (2012) found that TOC tends to decrease the P- and S-wave velocities, density, and Vp/Vs ratios, while increasing the velocity anisotropies. Lucier et al. (2011) showed that, in the Haynesville shale gas reservoir, the effect of gas saturation on the Vp-Vs relation is more significant than that of the TOC effects. Guo et al. (2013) modeled the Barnett shale brittleness index with self-consistent approximations and the Backus average through considering the degree of the preferred orientation of clay and kerogen particles. However, little work has considered the effects of organic matter maturation when modeling organic-rich shales.

In this study, we quantify maturity levels and set various parameters to simulate kerogen properties at immature, mature, and overmature stages to model the elastic properties of organic-rich shales. We strive to make the modeling consistent with the microstructure and composition of organic-rich shales. We propose a workflow of modeling organic-rich shales by using effective medium theory. We compare the modeling results of immature and mature shale with the measured data from the Bakken shale core samples, which also increase the credibility when modeling overmature shale. Factors such as mineral compositions, volume of TOC (VTOC), and maturity levels are analyzed and interpreted separately.

Workflow of modeling organic-rich shales

Step I: generate the fully aligned clay-fluid composite

We start by generating anisotropic clay-fluid structures. Hereby, we neglect the smectite-to-illite transformation during organic-rich shales compaction and maturation. Clay mineral particles are featured as hexagonal symmetry, which contain five independent elastic constants. We applied elastic stiffnesses used by Sayers (2013): C_{11} = 44.9 GPa, C_{33} = 24.2 GPa, C_{44} = 3.7 GPa, C_{66} = 11.6 GPa, and C_{13} = 18.1 GPa.

To create a biconnected solid at specific porosities (Figure 1), we can use an anisotropic version of the differential effective medium (DEM) method (Nishizawa, 1982). In the evolution history of organic-rich shales, clay minerals aggregate (suspension status) and start to be deposit with time, and the degree of compaction increases with time, leading to decrease porosity. We assume that the fluid in clay-related pores is brine. The DEM helps to preserve the connectivity of the clay solid phase, and the wet pores are treated as non-connected phase (inclusions) due to the low permeability of organic-rich shales as well as the unequilibrated pore pressure, when waves propagate

© 2014 SEG
DOI http://dx.doi.org/10.1190/segam2014-1584.1

Downloaded 09/11/14 to 98.201.57.71. Redistribution subject to SEG license or copyright; see Terms of Use at http://library.seg.org/

through. In this study, the aspect ratios of clay-related pores are set as 0.1 and can be linked with the relationship between pore shape and compaction.

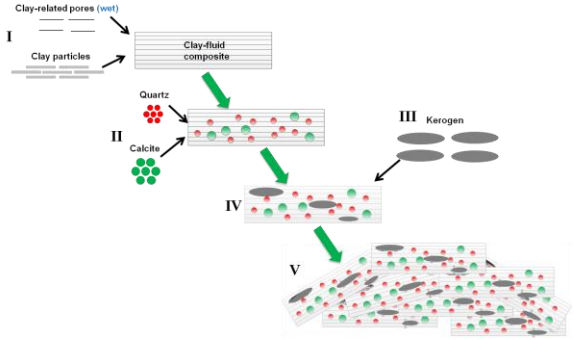

Figure 1. The workflow of modeling organic-rich shales.

Step II: include silt minerals in the generated clay-fluid composite

Silt-sized minerals (quartz, calcite, and pyrite) tend to exist as roughly spherical shapes that are randomly oriented, and their concentrations vary locally in unconventional shale plays. We can use anisotropic self-consistent approximation (ASCA) (Hornby et al., 1994) to include quartz and calcite in the clay-fluid composites to obtain the elastic properties of shale's inorganic part, as it is unnecessary to identify one of the minerals as the host and the other two as inclusions.

Step III: model organic matter properties with different maturity levels

Among numerous factors influencing the properties of organic-rich shales, organic matter is crucial because of its particular velocity, density, and maturation. During the process of organic matter maturation, various reactions take place at different maturity levels. The workflow of our rock physics modeling is modified for different maturity levels (Figure 2), where different values of densities and moduli of kerogen and the aspect ratio of kerogen-related pores are listed in Table 1.

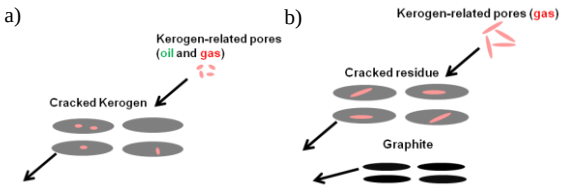

Figure 2. The modification for step III in Figure 1 when modeling organic matter for (a) mature and (b) overmature cases.

We consider organic matter as a system consisting of solid kerogen or a solid mixture of reaction residue with graphite, and kerogen-related pores filled with hydrocarbons (Figure 2) distributed in the organic matter. The substance phases and their volume fractions in the organic matter is referred to the maturation model of organic matter built with table 1 and 2 in Luo and Vasseur (1996). Since we can treat the organic system as an effective medium, the cracked kerogen elastic properties can be calculated using the self-consistent approximation (SCA) method (Mavko et al., 2009). For immature kerogen [Ro (%) < 0.6] (Vanorio et al., 2008), a bulk modulus of 3.5 GPa and a shear modulus of 1.75 GPa (Yan and Han, 2013) are applied. In this stage, the temperature of the formation is below 60°C, and little gas and few kerogen-related pores are generated. For mature kerogen [0.6 < Ro (%) < 1.3], pore fluid can be treated as a mixture of oil and gas, whose stiffness is calculated with Wood's (1955) relation, and the bulk and shear moduli of solid kerogen are 5 GPa and 2.5 GPa (Yan and Han, 2013), respectively. For overmature kerogen [Ro (%) > 1.3], the elastic properties of a solid mixture of kerogen and graphite can be calculated using the SCA method since we can suggest reasonable aspect ratios for these two materials based on the microstructure observed from scanning electron microscope (SEM) images. Furthermore, all the oil decomposes to form gas because of the higher temperature (> 150°C), and the fluid in kerogen-related pores is only gas. The elastic moduli of kerogen (Lucier et al., 2011) and graphite (Ruiz, 2009) are set at 7.98 GPa and 4.18 GPa and 4.79 GPa and 4.54 GPa, respectively.

Table 1. Elastic properties of kerogen with different maturity levels and the aspect ratio of kerogen-related pore utilized in the rock physics modeling.

Maturity Level	Hydrocarbon Composition	$K_{kerogen}$ (GPa)	$\mu_{kerogen}$ (GPa)	$\alpha_{\phi k}$
Immature	Oil	3.5	1.75	0.5
Mature	Oil and Gas	5	2.5	0.2
Overmature	Gas	7.98	4.18	0.1

Step IV: add organic matter in the former shale background

After the effective properties of organic matter with different maturity levels are generated, we can add cracked kerogen as an inclusion of the former shale matrix to simulate the properties of the organic-rich shale. In this step, the cracked kerogen inclusions are assumed to be aligned along the shale bedding (Figure 1). To preserve the connectivity of the rock matrix, an anisotropic version of the DEM method is applied.

Step V: average over the orientation distribution function

SEM images (Hornby et al., 1994; Alfred and Vernik 2012) of shales generally show that the clay aggregates' alignment varies in orientation but serves as a transverse isotropic (TI) medium as a whole, whose symmetry axis is

© 2014 SEG

DOI http://dx.doi.org/10.1190/segam2014-1584.1

Downloaded 09/11/14 to 98.201.57.71. Redistribution subject to SEG license or copyright; see Terms of Use at http://library.seg.org/

perpendicular to the bedding. Hornby et al. (1994) described the properties of the composite in terms of a complex solid comprised of a distribution of these particle aggregates. This study adopts this averaging strategy to add a particle distribution characteristic into the organic-rich shale model (Figure 1). Hornby et al. (1994) derived a distribution function of particle orientation from an SEM image. In our study, these particles' orientation distribution function adopts a discrete normal distribution.

Rock physics modeling results and analysis

Here we present our modeling results for mature organic-rich shales. Compared with immature organic-rich shales, organic matter becomes denser and stiffer when kerogen cracks to form oil and gas. The bulk and shear moduli of kerogen are set as 5 GPa and 2.5 GPa, respectively, and a density of 1.3 g/cc is applied. Based on the maturation model for type II kerogen (Luo and Vasseur, 1996), when organic-rich shale is cooked to mature status, the mass concentrations of the organic phase are 70% solid organic matter, 20% oil, and 10% gas. Hereby we make an assumption that kerogen and the solid residue generated during the decomposition of kerogen share the same elastic properties and density but different reaction activity energy, i.e. kerogen decompose totally before the organic-rich shale is heated to 120°C, but generated residue decompose when temperature reaches 150°C. The inorganic matrix of our model consists of a mineral combination of 25% quartz, 55% calcite, and 20% clay. The matrix porosity is 1%, and kerogen-related porosities vary from 0% to 8%, which are the modeling results of adjusting the densities of kerogen-related porosity. Some parameters used in the mature organic-rich shale model are listed in Table 2. We simulate the properties of mature organic-rich shales with different initial volume fractions of kerogen (VTOC) ranging from 5% to 45%. Figures 3 and 4 plot the modeling results and eight mature Bakken shale samples from Vernik and Nur (1992) with Ro (%) varying from 0.6 to 1.1, which are superimposed to check the feasibility and predictive power of the model.

Figure 3 shows that the modeling P- and S-wave (normal-to-bedding) velocities with different volume fraction of kerogen and kerogen-related porosity. The kerogen-related porosity ϕ_k can increase with the crack density of kerogen-related pores (black arrow), which indicates the maturity level. Since more kerogen is decomposed to form oil and gas, generating pores also contribute significantly to the total porosity, which can increase as high as 8% when initial VTOC is 45%. From the modeling results, higher kerogen volumes and kerogen-related porosities both decrease the P- and S-wave velocities. When the VTOC is the same, increasing maturity level can decrease P- and S-wave velocities. Eight Bakken shale samples data are plotted and marked with red stars. As a whole, they follow the trend, and most of them fall within the range of the predicted model in the panels of Vp-VTOC and Vs-VTOC.

Table 2. Parameters used in the mature organic-rich shale model.

Matrix porosity (ϕ_{nk})	1%	**K_{oil}**	0.48 GPa
Matrix-related pore aspect ratio (α_{nk})	0.1	**μ_{oil}**	0 GPa
Kerogen-related porosity (ϕ_k)	0-8%	**ρ_{oil}**	0.8 g/cc
Kerogen-related pore aspect ratio (α_k)	0.2	**K_{water}**	2.25 GPa
Kerogen aspect ratio (α_{kerogen})	0.1	**μ_{water}**	0 GPa
Clay aspect ratio (α_{clay})	0.1	**ρ_{water}**	1.04 g/cc
Gas to oil volume ratio in kerogen related pores	9	**K_{gas}**	0.01 GPa
Volume fraction of kerogen	5-45%	**μ_{gas}**	0 GPa
Crack density of kereogen-related pore	0-0.2	**ρ_{gas}**	0.1 g/cc

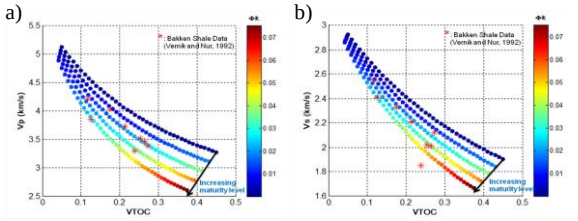

Figure 3. Rock physics modeling results for (a) P-wave velocity (Vp) and (b) S-wave velocity (Vs) vs. volume fraction of kerogen (VTOC) and kerogen-related porosity (ϕ_k) for mature organic-rich shales. Red stars denote the Bakken shale data with Ro (%) from 0.6 to 1.1 from Vernik and Nur (1992).

Kerogen is considered as an isotropic material, but its particle alignment, which is parallel to the shale bedding, can induce strong polar anisotropy. The modeled anisotropies results in the mature rock model are stronger than the modeled results in the immature rock model, resulting from differences in properties (such as stiffness and density, etc.) between the organic part and the inorganic part increasing during kerogen maturation. Organic matter becomes much softer than the rock matrix due to the generation of kerogen-related pores during maturation, and the anisotropy induced by bedding-aligned kerogen increases. Figure 4 demonstrates that, with increasing organic matter or maturity level, the Thomsen's parameters (Thomsen, 1986) increase. The reason why the

© 2014 SEG

DOI http://dx.doi.org/10.1190/segam2014-1584.1

Downloaded 09/11/14 to 98.201.57.71. Redistribution subject to SEG license or copyright; see Terms of Use at http://library.seg.org/

modeling results do not match well with the core data can be attributed to poor understanding of some microstructure information of particle alignments and improper aspect ratios setting for inclusions, such as clay-related pore, kerogen, etc.

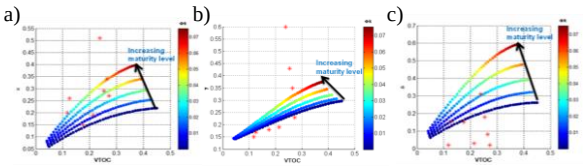

Figure4. Thomsen's parameters, (a) ε, (b) γ, and (c) δ vs. volumes fraction of kerogen (VTOC) and kerogen-related porositiy (ϕ_k).

Then we take a look at the Vp/Vs ratios of immature, mature, and overmature organic-rich shales with our rock physics modeling in Figure 5. In panel (a), the modeling kerogen-related porosity is lower than 1% since we are simulating oil shale and little kerogen decompose. For that core sample with a VTOC of 43%, the Vp/Vs value is as low as that of gas sand; this deviation may be explained with the unknown pore fluid saturation and inaccurate measurement if pore fluid remains in-situ status with a Ro of 0.3%. When the kerogen volume fraction is low (VTOC < 25%), the Vp/Vs ratio of organic-rich shales can decrease with increasing amount of organic matter. When VTOC is larger than 25%, the Vp/Vs ratio of organic-rich shales are close to 1.73 and do not change significantly.

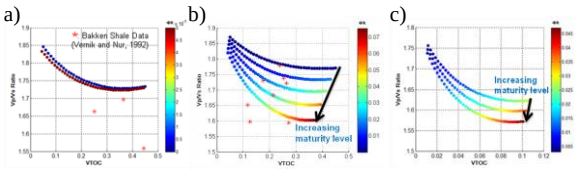

Figure 5. The rock physics modeling results for the Vp/Vs ratios of (a) immature, (b) mature, and (c) overmature organic-rich shales vs. volumes fraction of kerogen (VTOC) and kerogen-related porositiy (ϕ_k). Red stars in panel (a) and (b) denote the Bakken shale data with Ro (%) from 0 to 0.6 and from 0.6 to 1.1 from Vernik and Nur (1992).

In Figure 5b, the Vp/Vs ratios, which can be as low as 1.6, decrease significantly with increasing maturity levels (kerogen-related pores) or kerogen volumes. When the kerogen volume fraction is lower (VTOC < 25%), an increasing amount of kerogen mainly dominates the Vp/Vs ratio; when VTOC is larger than 25%, the increasing level of maturity mainly controls the decrease of the Vp/Vs ratio. In this case, the kerogen-related porosities are higher than those of the overmature case, because kerogen-related pores have larger aspect ratio but smaller crack density than those of overmature case, which suggests that the kerogen-related porosity can take a large proportion of the total porosity in mature organic-rich shales.

In Figure 5c, for the overmature case, we do not have data to check the predictive power. But we consistently follow the geology based workflow by adjusting several modeling parameters, such as compositions of organic matter phase, lower aspect ratio, and higher crack density of kerogen-related pores. The modeling Vp/Vs ratio can be as low as 1.57 since all of the fluid within the kerogen-related pores remains only gas at depths with temperatures over 150°C. The VTOC varies from 1% to 11% and is much less than the former two cases, although the initial VTOC is set as the same range of 5 to 45% with immature and mature cases. This is because at overmature stage, kerogen is totally decomposed, and the solid phase of organic matter consists of reaction residue as organic carbon and graphite as the inorganic carbon.

It is necessary to point out that the rock physics modeling contains amounts of parameters, which are assigned to represent the geochemical compositions, such as volume fractions of minerals and kerogen, and microstructures, such as inclusion geometries (aspect ratio), and distributions (orientation distribution function). We need to determine them properly so that the modeling results follow well with the in-situ geological characteristics of the organic-rich shales. One preferable method of setting parameters is to determine the mineral compositions with X-ray diffraction (XRD), TOC and maturity level with Rock-eval pyrolysis, and the microstructure with SEM figures.

Conclusions

It is essential to consider maturity level besides other geological factors when modeling organic-rich shales. We find that different maturity levels can affect elastic properties, such as the velocities, anisotropies, and Vp/Vs ratios, to different degrees. For immature shale with little kerogen-related pores, TOC is the major factor that determines its elastic responses. For mature shale, the elastic properties are mainly controlled by the maturity level of the organic matter. For overmature shale, the elastic properties are mainly determined by the gas-filled kerogen-related pores.

Acknowledgements

The authors would like to thank Fluids/DHI consortium for supporting the study. We also appreciate the assistance and valuable comments provided by Franklin Ruiz and colleagues at the Rock Physics Lab, Fuyong Yan, Qiuliang Yao, Hui Li, Hemin Yuan, and Malleswar Yenugu.

© 2014 SEG

DOI http://dx.doi.org/10.1190/segam2014-1584.1

http://dx.doi.org/10.1190/segam2014-1584.1

EDITED REFERENCES

Note: This reference list is a copy-edited version of the reference list submitted by the author. Reference lists for the 2014 SEG Technical Program Expanded Abstracts have been copy edited so that references provided with the online metadata for each paper will achieve a high degree of linking to cited sources that appear on the Web.

REFERENCES

Alfred, D., and L. Vernik, 2012, A new petrophysical model for organic-rich shales: 53rd Annual Logging Symposium, SPWLA, 16–20.

Carcione, J. M., and A. F. Gangi, 2000, Gas generation and overpressure: Effects on seismic attributes: Geophysics, **65**, 1769–1779, http://dx.doi.org/10.1190/1.1444861.

Carcione, J. M., H. B. Helle, and P. Avseth, 2011, Source-rock seismic-velocity models: Gassmann versus Backus: Geophysics, **76**, no. 5, N37–N45, http://dx.doi.org/10.1190/geo2010-0258.1.

Dræge, A., M. Jakobsen, and T. A. Johansen, 2006, Rock physics modeling of shale diagenesis: Petroleum Geoscience, **12**, no. 1, 49–57, http://dx.doi.org/10.1144/1354-079305-665.

Guo, Z., X. Li, C. Liu, X. Feng, and Y. Shen, 2013, A shale rock physics model for analysis of brittleness index, mineralogy, and porosity in the Barnett Shale: Journal of Geophysics and Engineering, **10**, no. 2, 1–11, http://dx.doi.org/10.1088/1742-2132/10/2/025006.

Lucier, A. M., R. Hofmann, and L. T. Bryndzia, 2011, Evaluation of variable gas saturation on acoustic log data from the Haynesville Shale gas play, NW Louisiana, USA: The Leading Edge, **30**, 300–311, http://dx.doi.org/10.1190/1.3567261.

Luo, X., and G. Vasseur, 1996, Geopressuring mechanism of organic matter cracking: Numerical modeling: AAPG Bulletin, **80**, no. 6, 856–874.

Mavko, G., T. Mukerji, and J. Dvorkin, 2009, The rock physics handbook: Cambridge University Press.

Nishizawa, O., 1982, Seismic velocity anisotropy in a medium containing oriented cracks: Journal of Physics of the Earth, **30**, no. 4, 331–347, http://dx.doi.org/10.4294/jpe1952.30.331.

Ruiz, F. J., 2009, Porous grain model and equivalent elastic medium approach for predicting effective elastic properties of sedimentary rocks: Ph.D. dissertation, Stanford University.

Sayers, C. M., 2013, The effect of anisotropy on the Young's moduli and Poisson's ratios of shales: Geophysical Prospecting, **61**, no. 2, 416–426, http://dx.doi.org/10.1111/j.1365-2478.2012.01130.x.

Thomsen, L., 1986, Weak elastic anisotropy: Geophysics, **51**, 1954–1966, http://dx.doi.org/10.1190/1.1442051.

Vanorio, T., T. Mukerji, and G. Mavko, 2008, Elastic anisotropy, maturity, and maceral microstructure in organic-rich shales: 78th Annual International Meeting, SEG, Expanded abstracts, 1635–1639.

Vernik, L., and X. Liu, 1997, Velocity anisotropy in shales: A petrophysical study: Geophysics, **62**, 521–532, http://dx.doi.org/10.1190/1.1444162.

Vernik, L., and J. Milovac, 2011, Rock physics of organic-rich shales: The Leading Edge, **30**, 318–323, http://dx.doi.org/10.1190/1.3567263.

Vernik, L., and A. Nur, 1992, Ultrasonic velocity and anisotropy of hydrocarbon source rocks: Geophysics, **57**, 727–735, http://dx.doi.org/10.1190/1.1443286.

Downloaded 09/11/14 to 98.201.57.71. Redistribution subject to SEG license or copyright; see Terms of Use at http://library.seg.org/

Wood, A. B., 1955, A textbook of sound: The physics of vibrations: Bell and Sons.

Yan, F., and D. Han, 2013, Measurement of elastic properties of kerogen: Presented at the 83rd Annual International Meeting, SEG.

Zhu, Y., S. Xu, M. Payne, A. Martinez, E. Liu, C. Harris, and K. Bandyopadhyay, 2012, Improved rock-physics model for shale gas reservoirs: 82nd Annual International Meeting, SEG, Expanded Abstracts, doi: 10.1190/segam2012-0927.1.

Downloaded 09/11/14 to 98.201.57.71. Redistribution subject to SEG license or copyright; see Terms of Use at http://library.seg.org/